

Ray-Tracing Wireless Channel Modeling and Verification in Coordinated Multi-Point Systems

Mohammad Amro, Adnan Landolsi, Salam Zummo
Electrical Engineering Department, KFUPM
31261 Dhahran, Saudi Arabia
mohammad.amro@ieee.org, {andalusi, zummo}@kfupm.edu.sa

Michael Grieger, Martin Danneberg, Gerhard Fettweis
Vodafone Chair Mobile Communications Systems
01069 Dresden, Germany
{michael.grieger, martin.danneberg, fettweis}@ifn.et.tu-dresden.de

Abstract— Coordinated Multi-Point (CoMP) Multiple Input Multiple Output (MIMO) transmission improves user's coverage and data throughput particularly on the cell edges. To make full advantage of CoMP, radio planning tools need very accurate models that fully capture the MIMO channels characteristics. This paper presents detailed modeling and analysis of an uplink CoMP system using Ray-Tracing (RT)-based channel modeling. The contribution of this paper is to show how close RT simulations can predict end-to-end system performance compared to the real-world measured performance. Thorough drive test measurements and RT simulations were performed. CoMP and Conventional MIMO systems performances are evaluated and compared for measured and RT-simulated channels. The results of several scenarios show that the RT matches the measurements in terms of rates and geometrical properties. The CoMP gain resulting from the measurements is almost double the gain of RT simulations. The differences come from the hardware and the RT 3D models impairments.

Keywords— Ray Tracing; Channel; Modeling; SNR; SINR; Coordinated Multi-Point; CoMP; Spectral Efficiency; LTE-Advanced

I. INTRODUCTION

The International Telecommunication Union (ITU) statistical report of Information and Communication Technology (ICT) issued on February, 2013 highlights that there are almost as many mobile subscriptions as people in the world, (around 7 billion) [1]. The traffic demand of new services is constantly increasing through data oriented wireless communications technologies, such as Universal Mobile Telecommunications System (UMTS), Worldwide interoperability for Microwave Access (WiMAX) and Long Term Evolution (LTE). The big obstacle facing this growth is the limited frequency spectrum, the most precious resource nowadays [2]. Therefore, novel techniques are required to increase spectral efficiency.

Coordinated Multi-Point (CoMP) communications (transmission and reception) is a hot research area and addressed by the Third Generation Project Partnership (3GPP) as a future mechanism for interference mitigation within radio interface in future LTE releases (release-10 and beyond), known as LTE-Advanced [3]-[5]. In [6], field measurements (FM) showed that CoMP could improve spectral efficiency by about 50% and cell-edge user throughput by about 55% compared to non-CoMP Conventional (Conv.) MIMO systems.

For efficient large-scale deployment of CoMP designs in commercial cellular networks, accurate predictions of propagation environments and system capacity have to be performed [7]. A well-known (deterministic) propagation prediction approach is the Ray Tracing (RT) model, which is receiving strong interest recently [8].

RT is a promising technique because it can capture a detailed characterization of all multipath components (MPCs), without any constraint concerning the antennas or the measurement equipment [9]. Therefore, RT models have the advantage of providing accurate site-specific information, which is easily reproducible without the need of on-site measurements or labor-intensive drive-test model tuning and correction [10]. As such, RT has been efficiently used in the design and performance simulation of different MIMO-based radio systems such as LTE and WiMAX [11].

In this paper, unlike previous works in the same testbed e.g. [12]-[14], the verifications of field-measured channels using RT simulated channels are introduced covering end-to-end performance analyses and comparisons. The results of both Conventional MIMO and CoMP systems are shown in terms of geometrical properties, SNR, and rates (SINR).

II. RAY TRACING (RT) SETUP

RT simulates output time delay, Direction of Arrival (DoA), Direction of Departure (DoD) and time variance of radio channels or Delay Spread (DS). Any RT simulation depends on basic physical principles, such as Maxwell's equations, Geometrical Optics (GO), Uniform Theory of Diffraction (UTD), and some efficiency increasing schemes. GO mainly refers to RT techniques that have been used for centuries at optical frequencies. 3D maps of a dense urban city are used which contain all major structures such as buildings and bridges and their construction materials such as permittivity coefficients, but still ignore the fine details such as trees, people and cars. During the RT simulation, rays are launched at the transmitter and propagate within the modeled environment until they hit a targeted receiver as shown in Fig. 1 or fall below a pre-specified noise floor level and are skipped [7]. RT model is capable of simulating multi-path propagation [7], [15] and [16].

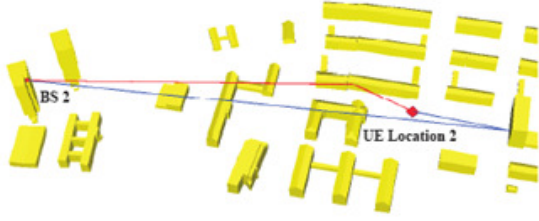


Fig. 1. Simulated field environment in RT with two rays [15].

In this work, the RT package Actix RPS 5.5 was used. A large number of parameters can influence the actual RT algorithm. A key parameter is the ray launching angular step size (in degrees) that determines the final number of rays that a transmitter will launch. We used a step size of one to achieve a best compromise between results accuracy and complexity. This is launched in two dimensions, azimuth, and tilt [15]. Channel Impulse Response (CIR) consists of all MPCs and represents their temporal and angular properties. Hence, RT CIR is double directional and given for a static channel by

$$\sum_{n=1}^N h_n(\vec{x}_{Tx}, \vec{x}_{Rx}, \tau, \phi, \psi) = \sum_{n=1}^N \alpha_n \cdot \delta(\tau - \tau_n) \cdot \delta(\phi - \phi_n) \cdot \delta(\theta - \theta_n) \quad (2)$$

where α_n, τ_n, ϕ_n and θ_n represent per MPC between a transmitter and a receiver (\vec{x}_{Tx} & \vec{x}_{Rx}) the complex amplitude, delay, azimuth and tilt respectively.

The RT model simulated the real testbed environment and has 16 Base Station (BSs) and two User Equipments (UEs) located at 887 different locations similar to the setup of the real field measurements locations. Each BS has one cross-polar antenna (two antenna elements) and each UE has one dipole antenna. Each CIR matrix represents all possible channels (launched paths) between a BS and a UE location. The UEs (transmitter) in the RT model are represented as grids or square areas. Fig. 2 shows the 3D map with grid areas representing the drive test route. The grid area needs to be designed carefully with a proper grid diameter. The bigger the diameter is the more the possibility to receive a ray and vice versa. Therefore, designing the grid needs to be matching the real world UE location. In the field measurements, the two UEs were installed on a measurement bus away from each other by 5 meters. This was considered in the grid design.

RT key parameters are shown in Table I, which were optimized based on iterative trials and believed to be reflecting the real propagation environments and the used hardware [15].

TABLE I. KEY PARAMETERS USED IN RT MODEL

Parameter	Configurations
Noise Floor (matching real hardware)	-100 dBm
Angular ray launching step	1°, (0.1°)*
Max. number of reflections	Infinite
Max. number of penetrations	4
Max. number of diffractions	3
Scattering model	Directive
Depolarization method	Mean
Buildings permittivity coefficient (real part)	5
Surface effective roughness	0.3
UE Inter-Distance	5 meters
Downtilts: UE1 / UE2	-76° / +42°
Azimuth UE1 / UE2	0° / +35°
UE (Transmitter) Grid Area	5 m ²

* Launching step of value 0.1 degrees was used in particular simulations

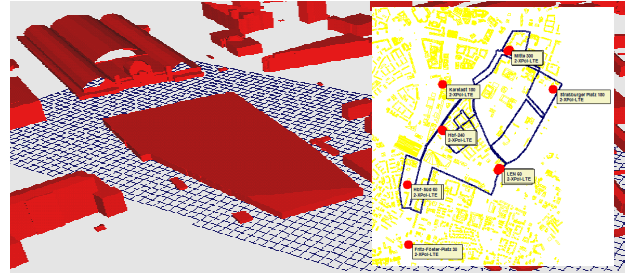


Fig. 2. Example of receiver grids implemented in a 3D model (Actix RPS), and the detailed route of grids simulating the drive test route.

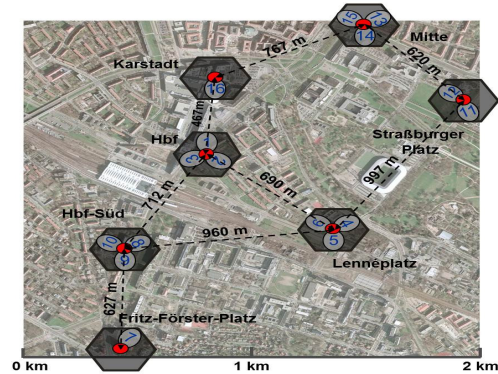
III. FIELD MEASUREMENTS (FM) SETUP

The field trial setup as modeled in RT setup is composed of 16 BSs deployed at seven UMTS co-sites in the downtown of the German city Dresden. Each BS is equipped with a cross-polarized antenna, hence two antenna elements per BS, the co-polar, and the cross-polar components. Two User Equipments (UEs) used; each had one linear vertical antenna [12]. Further parameters describing the trial testbed environment are in Table II.

TABLE II. TRANSMISSION PARAMETERS (SEE [14])

BS antenna height	30-55 m
Distance between UEs	about 5 m
UE antenna height (over the ground)	1.5 m
Carrier Frequency	2.53 GHz
System Bandwidth	20 MHz
Inter-BS distance	450-1000m

A measurement car that was traveling at a speed of around 7 km/h drove the route. The length of the measurement route is around 17 km. It passes through surroundings of very different building structures and vegetation. The FM collected at 887 locations distributed all over the testbed (Fig. 3.). The received signals at all BSs recorded for an offline evaluation [13].


 Fig. 3. Field trial setup, base stations distribution and measurements environment. Map data © Sandstein Neue Medien GmbH (<http://stadtplan.dresden.de>)

IV. RECEIVER TOOL CHAIN & SIGNAL PROCESSING

The UL transmitted FM are stored during the trial for further offline processing in the receiver tool chain (Fig. 4.). The RT simulated CIR is extracted pre-processed before being input to the same receiver tool chain. The receiver tool chain is emulating a receiver built on LTE architecture.

As a major difference, OFDM is used instead of SC-FDMA in the uplink transmission. The detailed signal processing architecture is described in [12] and [13].

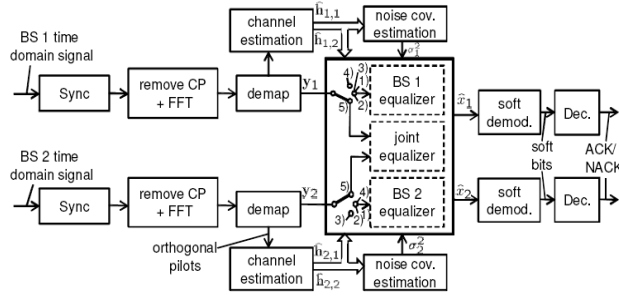


Fig. 4. Receiver tool chain – adapted from [13].

The signal processing architecture shown in Fig. 5, allows multiple cooperation and equalization schemes as:

- Independent decoding for both UEs by different BSs using interference rejection combining (IRC) shown in Fig. 5.a.
- Both UEs are decoded by the same BS, using a linear detector (IRC) shown in Fig. 5.b.
- One BS forwards its received signal to another BS(s), where both UEs are detected jointly (JD) using linear equalization shown in Fig. 5.c.

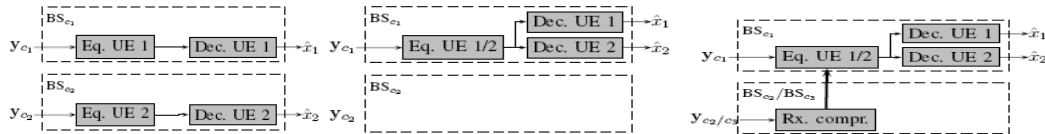
In a Conv. MIMO scheme, a local equalization is performed (e.g. MMSE) shown in Fig. 5.b, the BS corrects the scaling and phase rotation of the symbols as introduced by the channel. If UE n is locally detected at BS m , and subject to interference from UE $\bar{n} \neq n$, the biased MMSE filter for a particular sub-carrier is given as [12]

$$G_{\text{biased}}^{[m,n]} = \hat{h}_{m,n}^H (\hat{h}_{m,n} \hat{h}_{m,n}^H + \hat{h}_{m,\bar{n}} \hat{h}_{m,\bar{n}}^H + \hat{\sigma}_m^2 \mathbf{I})^{-1} \quad (3)$$

where $\hat{h}_{m,n}$ and $\hat{\sigma}_m^2$ are the estimates of the channel and noise. In case of JD CoMP shown in Fig. 5.c, an MMSE filter is used. If UE n is to be detected and still subject to the interference from UE $\bar{n} \neq n$, the biased MMSE filter for a particular sub-carrier is given as [12]

$$G_{\text{biased}}^{[n]} = \hat{h}_{C,n}^H (\hat{h}_{C,n} \hat{h}_{C,n}^H + \hat{h}_{C,\bar{n}} \hat{h}_{C,\bar{n}}^H + \text{diag}([\hat{\sigma}_{c1}^2 \mathbf{I} \dots \hat{\sigma}_{cC}^2 \mathbf{I}]))^{-1} \quad (4)$$

where $\hat{h}_{C,n}^H = [\hat{h}_{c1,n}^T \dots \hat{h}_{cC,n}^T]^T$ and $\hat{\sigma}_m^2$ are the estimates of the channel and noise, $\text{diag}(\cdot)$ takes a vector of size 2 to a diagonal matrix of size 2×2 , and $\text{diag}(\cdot)^{-1}$ maps the diagonal elements the entries of a size 2 vector.



(a) Both UEs decoded by different BSs. (b) Both UEs decoded by the same BS. (c) Joint Detection among 2 or 3 BSs

Fig. 5. Signal processing setup for Conv. MIMO schemes (a, b) and CoMP detection and cooperation schemes (c). See [13].

V. EVALUATION CRITERIA

A. Signal to Interference and Noise Ratio (SINR)

Linear filters were used in order to obtain post equalization SINR values. The filter minimizes the mean square error (MSE) and given by the Linear Mean Square Error (LMMSE) as:

$$G_{o,q} = (\mathbf{I} + \hat{\mathbf{H}}_{o,q}^H \Phi_{VV}^{-1} \hat{\mathbf{H}}_{o,q})^{-1} + \hat{\mathbf{H}}_{o,q}^H \Phi_{VV}^{-1} \quad (5)$$

where $\Phi_{VV} = ([\sigma_{v,1}^2 \dots \sigma_{v,M}^2])$. The post equalization SINR for the k^{th} user at the equalizer output ($\text{SINR}_{o,q}^k$) can be stated as

$$\text{SINR} = \frac{(\tilde{G}_{o,q}^k)^H \hat{\mathbf{H}}_{o,q}^k (\hat{\mathbf{H}}_{o,q}^k)^H \tilde{G}_{o,q}^k}{\sum_{i=1, i \neq k}^K (\tilde{G}_{o,q}^i)^H \hat{\mathbf{H}}_{o,q}^i (\hat{\mathbf{H}}_{o,q}^i)^H \tilde{G}_{o,q}^i + (\tilde{G}_{o,q}^k)^H \Phi_{VV} \tilde{G}_{o,q}^k} \quad (6)$$

where $\tilde{G}_{o,q}^k$ is the k^{th} column vector of matrix $\tilde{G}_{o,q} = G_{o,q}^H$.

Since the transmit signal is known under FM and RT simulations, the post-equalization SINR with the Error Vector Magnitude (EVM) estimation approach can be determined as

$$\text{SINR}_{o,q}^k \text{EVM} = E_{o,q} \{ |X_{o,q}^k - \hat{X}_{o,q}^k|^2 \} \quad (7)$$

where $\hat{X}_{o,q}^k$ is the estimation of the transmitted symbols.

B. Spectral Efficiency (Rate)

Based on SINR values the maximum achievable spectral efficiency assuming Gaussian noise is (R)

$$R = \sum_{k=1}^{n_t} \log_2(1 + \text{SINR}_k) \quad (8)$$

where SINR_k eq. (6) is used for theoretical rates and eq. (7) for EVM approach rates, where n_t is the number of transmitting antennas. SINR_k is the signal to interference plus noise ratio for the MIMO stream K .

C. CoMP Rate Gain and Matching Factor

To measure how much gain can CoMP techniques bring over the Conv. MIMO techniques we define a gain factor in terms of average spectral efficiencies (rates) as the percentage ratio between CoMP and Conv. schemes rates as

$$\text{CoMP Gain} = \frac{E\{\text{Rate}_{\text{CoMP}}\} - E\{\text{Rate}_{\text{Conv}}\}}{E\{\text{Rate}_{\text{Conv}}\}} \quad (9)$$

We defined also a matching factor comparing the average spectral efficiencies (rates) as the percentage ratio of the complement of the difference between the achieved rates using RT simulations and the rates using FM

$$\text{Matching Factor} = 1 - \left[\frac{E\{\text{Rate}_{\text{RT}}\} - E\{\text{Rate}_{\text{Meas}}\}}{E\{\text{Rate}_{\text{Meas}}\}} \right] \quad (10)$$

D. Propagation Geometries

1. Symbol Time Offset (STO):

As per 3GPP standards, UEs should be able to align their timing to all BSs of an intra-site cluster using LTE timing advance. This is difficult if the cooperation cluster is formed across sites (inter-site CoMP). Thus, larger symbol timing offsets (STOs) are expected. In order to avoid Inter-Symbol-Interference (ISI) the maximum delay should not exceed the cyclic prefix (CP) which is equal to 4.7 μs .

$$\text{Symbol Timing Offset (STO)} = \lceil \tau_d / T_s \rceil \quad (11)$$

where τ_d is the propagation delay and T_s is the sampling period. We assume that the STOs should be always less than or equal to the cyclic prefix duration (T_{CP}) minus a propagation delay (τ_d).

$$\text{STO} \leq (T_{\text{CP}} - \tau_d) \quad (12)$$

2. Time Difference Of Arrival (TDOA):

Due to the relatively small inter-site distances within the FM testbed, it is expected that the TDOA does not exceed T_{CP} . The geometrical TDOA is the difference in propagation time to all BSs in the cooperation cluster. Notice that the DS difference from multiple paths in such a testbed is very small (negligible), therefore a simplified TDOA formula can be approximated as

$$\text{TDOA} = \frac{\max(D) - \min(D)}{C_{\text{light}}} \quad (13)$$

where $D = [d_1 d_2]$, $d_k = [d_{c1,k} d_{c2,k}]$ is the distance between UE k and BSs $c1$ and $c2$ at any time. C_{light} is the speed of light.

VI. MODELING AND PERFORMANCE COMPARISON RESULTS

During FM UEs were not transmitting at the same time but with a delay interval that equals to 34 OFDM samples (about 1 μs). To simulate this behavior we padded 34 zeros for CIRs which could guarantee that UE2 is idle for 34 samples while UE1 is transmitting. This adaptation is called Sample Time Offset (SATO). Fig. 6 illustrates the design of SATO offset.

...	CIR_UE1	CIR_UE1	Padding zeros	CIR_UE1	CIR_UE1	Padding zeros	...
...	Padding zeros	CIR_UE2	CIR_UE2	Padding zeros	CIR_UE2	CIR_UE2	...

Fig. 6. SATO adaptation in RT by padding zeros to the resulting CIR

We observed during FM that the real hardware could measure SNR values between -5 dB and 33 dB, while RT simulator could detect SNR values between -10 dB and 43 dB. Real hardware limitations caused the limitations in FM.

Figure 7. shows the SNR CDF comparisons for all 16 BSs aggregated for all locations for both FM and RT simulations. We see that the introduction of SATO improves the matching accuracy between FM and RT channels.

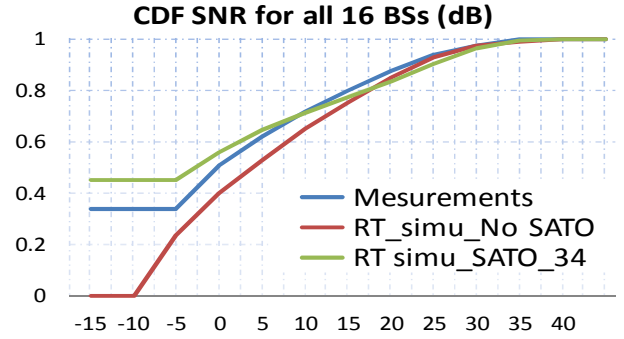


Fig. 7. CDF SNR values for all 16 BSs (Meas. and RT simu with and without SATO)

We compared the transmission rates for 12 scenarios summarized in Table III. The scenarios are composed of Conv. MIMO and CoMP schemes for both FM and RT simulations, applying Theoretical (Theo) and EVM approaches. Theo approach refers to using SINR eq. (6) and EVM approach refers to using SINR eq. (7). CoMP technique covers intra-site and inter-site. Intra-site CoMP indicates that the cooperating BSs belong to the same site while inter-site CoMP indicates that the cooperating BSs belong to different sites. Due to the paper length limitation the SIC results are not presented which are scenarios 7 to 12.

TABLE III. 12 MIMO COMPARISON SCENARIOS.

Scenario No.	Conv. MIMO &	Intra-CoMP &	Inter-CoMP &
1, 2, 3	EVM	EVM	EVM
4, 5, 6	Theoretical	Theoretical	Theoretical
7, 8, 9	EVM_SIC	EVM_SIC	EVM_SIC
10, 11, 12	Theoretical_SIC	Theoretical_SIC	Theoretical_SIC

Table IV shows the statistical values for the considered scenarios.

TABLE IV. STATISTICAL EVALUATION FOR SPECTRAL EFFICIENCY VALUES WITH DIFFERENT MIMO SCENARIOS.

No.	MIMO Scenario	Mean (bpcu)	STD (bpcu)	Median (bpcu)	Mean (bpcu)	STD (bpcu)	Median (bpcu)
1	Conv_Theo_MIMO	5.66	2.25	5.7	7.6	2.78	7.55
2	Intra_Theo_CoMP	6.6	2.06	6.57	8.23	2.77	8.57
3	Inter_Theo_CoMP	8.01	2	7.95	8.97	2.66	9.31
4	Conv_EVM_MIMO	4.6	1.77	4.75	6.6	2.42	6.6
5	Intra_EVM_CoMP	4.93	1.74	5.05	7.21	2.58	7.77
6	Inter_EVM_CoMP	6.13	1.4	6.2	7.59	2.25	8.09

Fig. 8.a, presents the rate gain ratios for CoMP scheme over Conv. MIMO scheme. Interestingly, the gain for RT simulations is comparable regardless which approach was used, Theo or EVM. The CoMP gain ratios in FM were higher when the Theo approach was used compared to the EVM approach. This indicates the errors coming during real world FM which are not happening in the RT (e.g. estimation errors).

FM rates are showing higher CoMP gain around 43% while RT CoMP gain is around 18%. The rates gain difference between Theo and EVM approaches was 10% for FM and 5% for RT.

Fig. 8.b. presents the matching factor, which reflects the similarity between RT and FM rates for both CoMP and Conv. MIMO schemes. RT simulations rates matched FM rates at the inter-site CoMP scenario by 88%. This high matching can be explained by the fact that in the inter-site CoMP scenario the received signals are more diversified and coming from different non-collocated BSs. The major objects in the propagation environment mainly influence these signals. On the contrary, the lowest matching scenario with 53% was the intra-site CoMP. This low matching is explained by the fact that the intra-site CoMP scenario the received signals have less diversity and coming from collocated BSs. Moreover, comparing the overall SINR values for both FM and RT simulations for the 887 transmitter locations, the standard deviation value was about 4 dB, but based on comparing each location we could see that around 15% of RT simulation results did not match the FM. These locations in reality are located at trees alleys and heavy foliage but not modeled in the RT simulator and the fast fading properties were not captured.

Fig. 9 presents the rates CDFs for the considered MIMO scenarios. As expected, the inter-site CoMP achieved higher spectral efficiencies for both FM and RT followed by intra-site CoMP and at last by the Conv. MIMO results. RT simulation rates could achieve higher rates than the ones resulting from FM. The CDF of STO for both FM and RT for cooperation clusters of two BSs shown in Fig. 10. The STO values for intra-site cooperation are, as expected, lower than the ones for inter-site cooperation due to the bigger distance in case of the inter-site cluster. Furthermore, the results indicate that a large percentage of the STOs are within the CP. Therefore, this guarantees that no ISI could have occurred.

In addition, it is shown that the STO for intra-site clusters is shorter than the STO for inter-site clusters by around 1 μ s. As we see in Fig. 10, almost all LOS TDOA were arriving within the CP time.

VII. CONCLUSIONS

RT simulation is a promising radio planning and propagation prediction technique that captures CoMP real-world measurements. RT simulations require proper modeling for RT algorithms and high accuracy 3D maps. A key parameter in RT modeling is the design of the ray launching step size that requires a compromise between accuracy and simulations time and the UE grid size. Inter-site CoMP showed less sensitivity to RT modeling errors while Conv. MIMO and Intra-Site CoMP were more sensitive. RT Simulations showed less CoMP gain compared to FM gain. The real hardware estimation errors and the shortage of very detailed 3D objects in the RT model reduced the matching between FM and RT simulations results. The deviations come from real hardware errors Field measurements rates show high CoMP gain by around 43%, while RT CoMP gain is around 18%. Field measurements had 10% higher rates when using theoretical post-equalization schemes compared to Error Vector Magnitude (EVM) rates, while RT rates had around 5%. Geometrical analyses showed that an Inter-Carrier-Interference (ICI) is unlikely due to short inter-site distance in the testbed. Inter-Site CoMP showed higher gain compared to intra-site. RT simulations could simulate the geometrical characteristics measured in real radio environment.

ACKNOWLEDGMENT

We would like to thank Carsten Jandura and Jens Voigt from Actix GmbH for their support during this work.

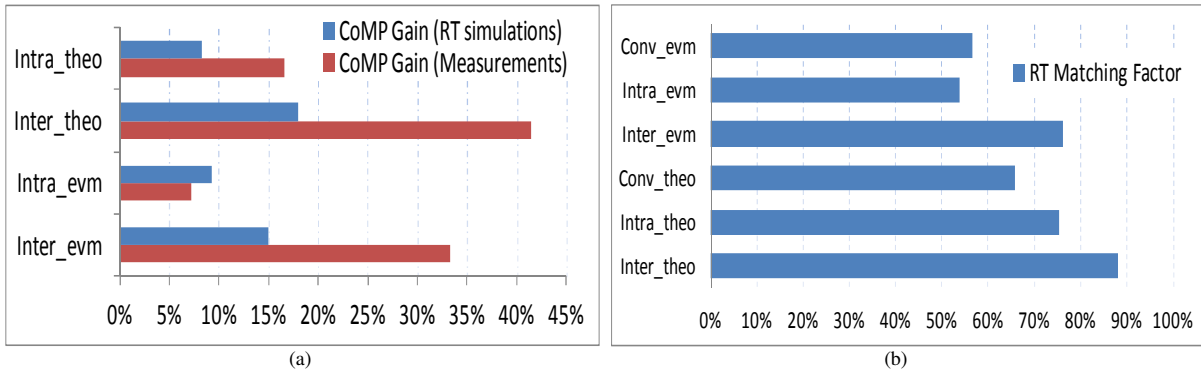


Fig. 8. (a) Spectral Efficiency (Rate) Gain comparing CoMP with Conv. MIMO with and without EVM approach for both RT simulations and FM. (b) RT simulation rates matching factor with FM rates when comparing the same MIMO scheme with and without EVM approach.

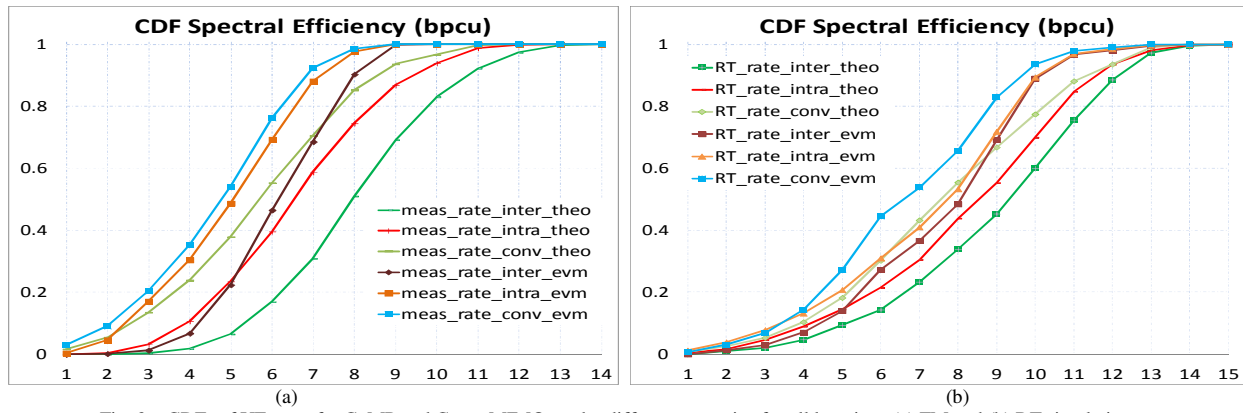


Fig. 9. CDFs of UE rates for CoMP and Conv. MIMO under different scenarios for all locations (a) FM and (b) RT simulations.

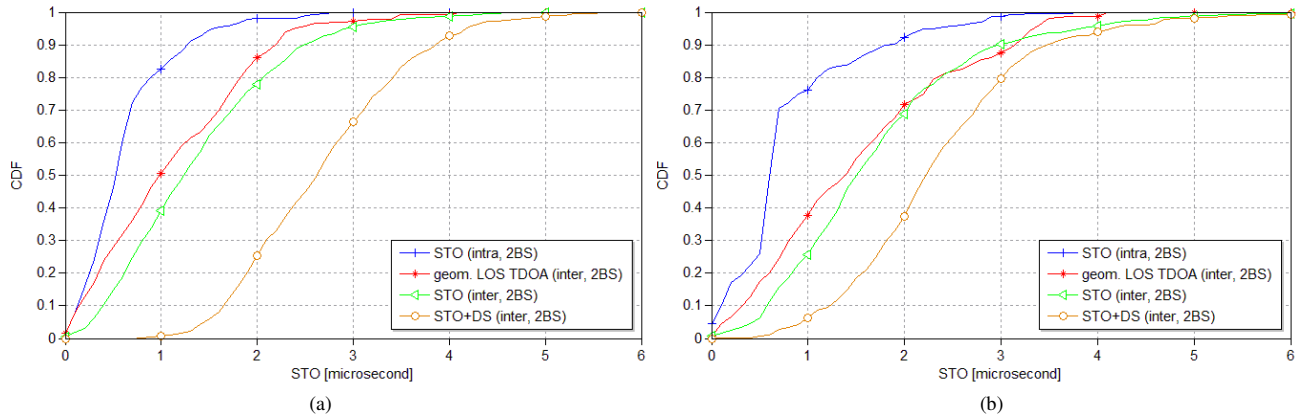


Fig. 10. CDFs for STO (intra-site and inter-site), Geometrical TDOA and DS (inter-site) for (a) FM and (b) RT simulations.

REFERENCES

[1] The World in 2013: ICT Facts and Figures, International Telecommunication Union (ITU), 27, February 2013. [Online]. [http://\[15\].itu.int/ITU-D/ict/facts/material/ICTFactsFigures2013.pdf](http://[15].itu.int/ITU-D/ict/facts/material/ICTFactsFigures2013.pdf)

[2] M.C. Necker, "Towards frequency reuse 1 cellular FDM/TDM systems", in Proceedings of 9th ACM/IEEE International Symposium on Modeling, Analysis and Simulation of Wireless and Mobile Systems (MSWiM 2006), Oct. 2006.

[3] 3GPP RP-090939 (3GPP Submission Package for IMT-Advanced), October 2009. [Online]. [http://\[15\].3gpp.org/ftp/tsg_ran/TSG_RAN/TSGR_45/Documents/RP-090739.zip](http://[15].3gpp.org/ftp/tsg_ran/TSG_RAN/TSGR_45/Documents/RP-090739.zip)

[4] S. Parkvall, E. Dahlman, A. Furuskar, Y. Jading, M. Olsson, S. Wanstedt, and K. Zangi, "LTE-Advanced - Evolving LTE towards IMT-advanced", in Proceedings of the 68th IEEE Vehicular Technology Conference (VTC'08 Fall), pp. 1-5, 2008.

[5] E. Dahlman, S. Parkvall, J. Skold, "4G: LTE/LTE-Advanced for Mobile Broadband: The 4G Solution for Mobile Broadband", Academic Press, Mar. 2011

[6] Irmer, R., Droste, H., Marsch, P., Grieger, M., Fettweis, G., Brueck, S., Mayer, H.-P., Thiele, L., Jungnickel, V., "Coordinated multipoint: Concepts, performance, and field trial results", in Proceedings of the IEEE Communications Magazine, Feb. 2011.

[7] Iskander, M.F., Zhengqing Yun, "Propagation prediction models for wireless communication systems", in Proceedings of IEEE Journal for Microwave Theory and Techniques, IEEE Transactions, Mar. 2002.

[8] V. Degli-Esposti, F. Fuschini, E. Vitucci, and G. Falciasecca, "Speed-Up Techniques for Ray Tracing Field Prediction Models," IEEE Transactions on Antennas and Propagation, Vol. 57. pp. 1469-1480. May 2009.

[9] Fugen, T., J. Maurer, W. Sorgel, and W. Wiesbeck, "Characterization of multipath clusters with ray-tracing in urban MIMO propagation environments at 2 GHz", IEEE Proceedings of the International Symposium on Antennas and Propagation, Washington DC, USA, 2005.

[10] M. Amro, M.A. Landolsi, S.A. Zummo, "Practical verifications for coverage and capacity predictions and simulations in real-world cellular UMTS networks," International Conference on Computer and Communication Engineering (ICCC), vol., no., pp.174-179, 3-5 2012.

[11] Y. Corre and Y. Lostanlen, "3D urban propagation model for large ray-tracing computation," in Proceedings of the International Conference on Electromagnetics in Advanced Applications (ICEAA '07), pp. 399-402, Torino, Italy, September 2007.

[12] Michael Grieger, Gerhard Fettweis, Patrick Marsch, "Large Scale Field Trial Results on Uplink CoMP with Multi Antenna Base Stations", in Proceedings of the IEEE Vehicular Technology Conference (VTC Fall), Sept. 2011.

[13] Grieger, M., Marsch, P., Zhijun Rong, Fettweis, G., "Field trial results for a coordinated multi-point (CoMP) uplink in cellular systems", IEEE Smart Antennas (WSA), International ITG Workshop on, Feb. 2010.

[14] M. Grieger, V. Kotsch, G. Fettweis, "Comparison of intra and inter site coordinated joint detection in a cellular field trial", Personal Indoor and Mobile Radio Communications (PIMRC), 2012 IEEE 23rd International Symposium.

[15] M. Danneberg, J. Holfeld, M. Grieger, M. Amro and G. Fettweis, "Field Trial Evaluation of UE Specific Antenna Downtilt in an LTE Downlink," in Proceedings of the 16th International ITG Workshop on Smart Antennas (WSA2012), Mar. 2012, Germany.

[16] C. Cerasoli, "The Use of Ray Tracing Models to Predict MIMO Performance in Urban Environments," in Military Communications Conference, 2006. MILCOM 2006. IEEE, oct. 2006.